



## The TeV Energy Spectrum of Mrk 421 Measured in A High Flaring State

A. KONOPELKO<sup>1</sup>, W. CUI<sup>1</sup>, C. DUKE<sup>2</sup>, J.P FINLEY<sup>1</sup>

<sup>1</sup>*Purdue University, Department of Physics, 525 Northwestern Avenue, West Lafayette, IN 47907-2036,*

<sup>2</sup>*Grinnell College, Department of Physics, 1116 8th Ave, Grinnell, IA 50112-1690*

*akonopel@purdue.edu*

**Abstract:** The BL Lac object (blazar) Mrk 421 was observed during its outburst in April 2004 with the Whipple 10 m telescope for a total of about 24.5 hours. The measured  $\gamma$ -ray rate varied substantially over the range from 4 to 10  $\gamma$ 's/min and eventually exceeded the steady  $\gamma$ -ray rate of the Crab Nebula (standard candle) by a factor of 3. The overall significance of the  $\gamma$ -ray signal exceeded  $70\sigma$  and the total number of excess events was more than 10,000. The signal light curve does not show any particular variability pattern. This unique Mrk 421 outburst enabled the measurement of a high quality spectrum of very high-energy  $\gamma$  rays in a high state of emission. This spectrum is a power-law and it extends beyond 10 TeV.

### Introduction

Mkn 421 is the first detected, the closest known (red shift  $z = 0.030$ ), and one of the best studied TeV  $\gamma$ -ray emitting blazars. The very high-energy (VHE)  $\gamma$ -ray emission arises from the particles accelerated in a relativistic jet directed along our line-of-sight. Since its discovery, Mkn 421 has shown very low baseline TeV  $\gamma$ -ray emission with a few extremely rapid flares on time-scales from one day to 15 minutes [7]. In 2000 and 2001 Mkn 421 went into a flare state with an average flux of 4 times that of the Crab Nebula. Data taken during this flare have been used to extract the energy spectrum at high energies, up to 20 TeV. Noticeable variations in the hardness of the TeV  $\gamma$ -ray energy spectrum have been reported [1, 12]. A number of successful multi-wavelength campaigns for Mkn 421 have revealed evidence of a correlation of the simultaneously measured fluxes in X-ray and TeV  $\gamma$ -ray energy bands [11, 4].

A one-zone synchrotron-self-Compton (SSC) model described the observational results reasonably well (e.g., [10]). During April 2004, an intensive multi-wavelength monitoring campaign on the TeV blazar Mkn 421 has been performed simultaneously in radio, optical, X-ray, and  $\gamma$  rays. The source was seen to be active in X-rays and TeV  $\gamma$  rays with the peak flux exceeding

the 3 Crab level [4]. The time-averaged energy spectrum of Mkn 421 during the flaring state has been measured at high energies with H.E.S.S. using large zenith angles observations [2], and MAGIC [3]. The Whipple 10 m telescope was observing Mkn 421 extensively during the April 2004 flare. Here we report the results on the TeV  $\gamma$ -ray energy spectrum of Mkn 421 measured in a high flaring state during the April 2004 outburst with the Whipple 10 m telescope.

### The 10 m Whipple Telescope

The reflector of the Whipple Observatory imaging atmospheric Cherenkov telescope (IACT) (see Figure 1) is a tessellated structure consisting of 248 spherical mirrors, which are hexagonal in shape and 61 cm from apex to apex, arranged in a hexagonal pattern. The mirrors are mounted on a steel support structure, which has a 7.3 m radius of curvature with a 10 m aperture. Each individual mirror has  $\sim 14.6$  m radius of curvature and is pointed toward a position along the optical axis at 14.6 m from the reflector. This arrangement constitutes a Davies, Cotton design [5] of the optical reflector. The point-spread function of the telescope has a FWHM of  $\sim 7.2'$  on-axis.

In 1999, a high-resolution camera (GRANITE III) was installed at the telescope [6]. It consists



Figure 1: Whipple Observatory 10 m Telescope at Mount Hopkins, Arizona.

of 379 photo-multiplier tubes (PMTs) in a close packed hexagonal arrangement (each PMT subtending  $0.11^\circ$  on the sky) and has a  $2.6^\circ$  diameter. A set of light concentrators is mounted in front of the pixels to increase the light-collection efficiency by  $\sim 38\%$ . The camera triggers if the signal in each of at least 3 neighboring PMTs out of the inner 331 exceeds a threshold of 32 mV, corresponding to  $\sim 8$ -10 photo-electrons. The post-GRANITE III upgrade trigger rate of the Whipple Observatory 10 m telescope is  $\sim 20$ -30 Hz at zenith.

## Observations & Analysis

Mkn 421 was observed with the Whipple Observatory 10 m IACT for about 24.5 hours of on-source data between April 9th and April 23d, 2004. Data have been taken in good weather at zenith angles less than  $30^\circ$  (mean elevation is about  $75^\circ$ ). During observations the raw detection rate was about 22 Hz. Observations have been performed using tracking mode in data runs of 28 minutes each. The recorded images are first flat-fielded using nightly measured nitrogen arc lamp PMT responses and then cleaned by applying a standard picture and boundary technique with canonical thresholds of 4.25 and 2.25 times the standard deviation of the PMT pedestal distributions, respectively (see, e.g., [9]). To characterize the shape and orientation of calibrated images, the standard second-moment image parameters are calculated as described in [16]. The *CAnalyze* package developed at Purdue University [13] is used for the primary data

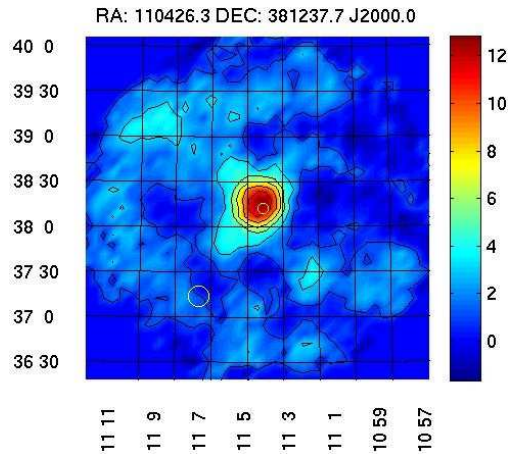


Figure 2: The two-dimensional map of excess significances over the sky region around Mkn 421 generated for the data sample corresponding to a high emission state. The map of uncorrelated rectangular angular bins of a  $0.1^\circ$  size has been smoothed using Gaussian kernel with the angular size of  $0.22^\circ$ . The maximal significance of  $\gamma$ -ray excess using this analysis is  $12.3\sigma$ .

Table 1: *Supercuts* selection criteria for the Whipple Observatory 10 m telescope (*dc* stands for digital counts).

Quantity	Image Parameter Cut
Trigger	1st & 2nd brightest pixel $> 30$ dc
Shape	$0.05^\circ < width < 0.12^\circ$ $0.13^\circ < length < 0.25^\circ$
Muon cut	$length/size < 0.0004$ ( $^\circ$ dc $^{-1}$ )
Quality cut	$0.4^\circ < distance < 1.0^\circ$
Orientation	$\alpha < 15^\circ$

analysis. Analysis methods known as Supercuts (see Table 1) and extended Supercuts are applied for the  $\gamma$ -ray/hadron separation. The latter utilizes dynamic, energy dependent orientation and shape cuts. The significance map of the sky region around Mkn 421 for the data set corresponding to a high emission state (exposure of 55 minutes) is shown in Figure 3. The energy spectrum of Mkn 421 is reconstructed using algorithms described in [15].

## Simulations

The KASCADE shower simulation code [8] is used for generating the  $\gamma$ -ray and cosmic-ray in-

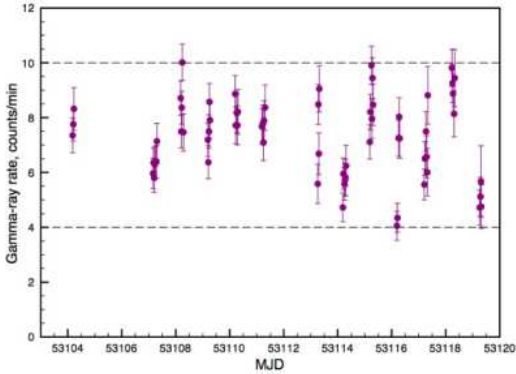


Figure 3: Light curve of TeV  $\gamma$ -ray emission from Mkn 421 during its outburst in April 2004.

duced air showers within the corresponding range of zenith angles and in the primary energy range between 50 GeV and 100 TeV, assuming the  $\gamma$ -ray energy spectrum to be a power-law of 2.5. Simulations of the response of the Whipple Observatory 10 m telescope are carried out using the *GrISU* code, developed by the Grinnell College and Iowa State University groups.

## Results

The light curve of Mkn 421, measured with the Whipple Observatory 10 m telescope during the outburst in April 2004, does not reveal any particular pattern (see Figure 2). Two data runs with a flux above 3 Crab and an exposure of 55 minutes give exceptionally high  $\gamma$ -ray rate with an average value of  $9.85 \text{ min}^{-1}$  and a total of 545 excess counts. This excess corresponds to a significance of the  $\gamma$ -ray signal at a level of  $16.4 \sigma$ . The corresponding  $\gamma$ -ray energy spectrum is consistent with a pure power-law of index 2.66. This spectrum does not indicate any apparent gradual change of slope (see Figure 4). Such unusual behavior of the Mkn 421 TeV  $\gamma$ -ray spectrum measured in a high emission state suggests that the previously observed curvature in Mkn 421  $\gamma$ -ray spectrum is an intrinsic feature of the source rather than the footprint of  $\gamma$ -ray absorption by interacting with the soft photons of extragalactic background light.

## Modeling

To model the multi-wavelength spectrum of the BL Lac object Mkn 421 in a homogeneous Syn-

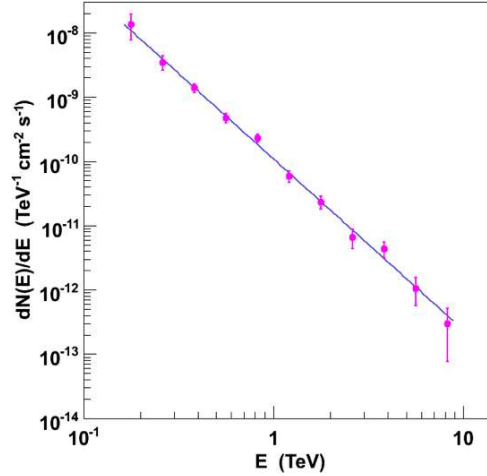


Figure 4: The energy spectrum of Mkn 421 measured in a high emission state during the outburst in April 2004.

chrotron Self Compton (SSC) scenario we use an approach described in [14]. This method involves prescribing an injection function for relativistic electrons and solving the two time-dependent kinetic equations for the electron and photon distributions of the source. All relevant physical processes are taken into account in the code, i.e., synchrotron radiation, inverse Compton scattering, photon-photon pair production, and synchrotron self-absorption. Seven model parameters are required to specify a source in a stationary state. These are the Doppler factor  $\delta$ , the radius  $R$  of the source, the magnetic field strength  $B$ , the index  $s$  of the electron injection spectrum, the Lorentz factor at the cut-off of the injection spectrum  $\gamma_{max}$ , the amplitude of the injection spectrum  $q_e$ , and the effective escape time of relativistic electrons  $t_{esc}$ . To optimize a fit to a particular data set, we used physically motivated starting values for these seven parameters (see [10]). This is done by identifying six scalars characterizing the blazar spectrum, the peak frequency  $\nu_{sync}$  of the synchrotron emission, the peak frequency  $\nu_{compt}$  of the inverse Compton emission, the total nonthermal luminosity  $L$ , the approximate ratio  $\eta$  of the total flux in the inverse Compton part to that in the synchrotron part of the spectrum, the break frequency  $\nu_{break}$ , the low-frequency spectral index, and finally the fastest variability timescale  $t_{var}$ . These observables enable one to find reasonable starting values of the

Table 2: Summary of Mkn 421 data analyzed by standard supercuts criteria (see Table 1.)

	Time [min]	ON	OFF	Excess	$R_\gamma \text{ min}^{-1}$	S/N [ $\sigma$ ]
April 2004	1472	18383	6872	11511	7.82	71.82
High state	55	825	280	545	9.85	16.40

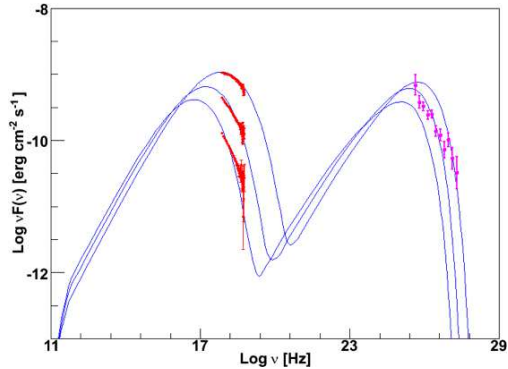


Figure 5: The spectral energy distribution of the Mkn 421 emission. The X-ray data, corresponding to low, medium, and high emission states have been taken from [4].

seven parameters of the SSC model. Using this approach we tried to fit the measured spectral energy distribution for a high state of Mkn 421. Despite that the X-ray spectra can be reasonably well reproduced by the one-zone SSC model, it does not provide a satisfactory fit to the TeV  $\gamma$ -ray spectrum of Mkn 421 measured in a high emission state (see Figure 5). It is worth noting that unfolding the TeV  $\gamma$ -ray spectrum from the IR absorption (see [10] for further details) yields an energy spectrum substantially harder than the measured one, which is more difficult to interpret in the framework of the one-zone SSC model.

## Discussion

Observations of Mkn 421 with Whipple [12] and HEGRA [1] during its historical flare in 2000 and 2001 have been used to extract the energy spectrum at high energies, up to 20 TeV. As stated by both groups, the energy spectrum of Mkn 421 is evidently curved. Analysis of the data revealed significant variations of the spectral slope at energies below 3 TeV depending on the emission state. However the best empirical fit to the data taken in both the high and the low states gives the same cut-

off energy of about 3.6 TeV. Recently, the gradual steepening in the Mkn 421 TeV energy spectrum was evidently detected with HESS [2] and MAGIC [3] during their 2004 and 2005 observational campaigns. This is consistent with the assumption that all Mkn 421 spectra are affected by intergalactic absorption. Here we report on the TeV  $\gamma$ -ray spectrum as measured with the Whipple 10 m telescope during a high emission state (at the flux level of 3 Crab), which does not indicate a cut-off feature in multi-TeV energy range and can be well-fitted by a pure power-law. Such an unusual spectrum indicates that the curvature could be an intrinsic feature of the source. This spectrum offers a challenge for the one-zone SSC model, and it may severely constrain the spectral energy distribution of extragalactic background light, which is the subject of a forthcoming refereed publication.

## References

- [1] F. Aharonian et al. *A&A*, 393:89, 2002.
- [2] F. Aharonian et al. *A&A*, 437:95, 2005.
- [3] J. Albert et al. *ApJ*, 663:125, 2007.
- [4] H. Blazejowski et al. *ApJ*, 630:130, 2005.
- [5] J. Davies and E. Cotton. *J. Soc. Energy*, 1:16, 1957.
- [6] J.P. Finley et al. *Proc. 27th ICRC*, 2827, 2001.
- [7] J. Gaidos et al. *Nature*, 383:319, 1996.
- [8] M. Kertzmann and G. Sembroski. *NIM*, A343:629, 1994.
- [9] J. Kildea et al. *Astropart. Phys.*, in press.
- [10] A. Konopelko et al. *ApJ*, 597:851, 2003.
- [11] H. Krawczynski et al. *ApJ*, 559:187, 2001.
- [12] F. Krennrich et al. *ApJ*, 575:L9, 2002.
- [13] R. Lessard et al. *Astropart. Phys.*, 19:221, 2001.
- [14] A. Mastichiadis and J. Kirk. *A&A*, 320:19, 1997.
- [15] G. Mohanty et al. *Astropart. Phys.*, 9:15, 1998.
- [16] P.T. Reynolds et al. *ApJ*, 404:206, 1993.